

# Polarization quantum beat spectroscopy of HCF( $\tilde{A}^1A''$ ).

## II. Renner–Teller and spin–orbit mixing in the simplest singlet carbene

Ionela Ionescu, Haiyan Fan, Eduard Ionescu, and Scott A. Reid<sup>a)</sup>  
*Department of Chemistry, Marquette University, Milwaukee, Wisconsin 53201*

(Received 2 July 2004; accepted 13 August 2004)

To further investigate the Renner–Teller (RT) effect and spin–orbit mixing in the  $\tilde{A}^1A'' \leftarrow \tilde{X}^1A'$  system of the simplest singlet carbene, HCF, we report a detailed analysis of the  $K_a = 1 \leftarrow 0$  subband of  $2_0^4$  using polarization quantum beat spectroscopy in combination with fluorescence excitation spectroscopy and lifetime measurements. This subband is perturbed both by RT and spin–orbit interactions, which are clearly differentiated due to the order-of-magnitude difference in matrix elements. We show that RT induced mixing with a high vibrational level of  $\tilde{X}^1A'$  leads to a splitting of this subband, and while the higher energy member is rotationally unperturbed, every line in the lower energy member is perturbed by spin–orbit mixing with background levels of  $\tilde{a}^3A''$ , as evidenced by large  $^{19}\text{F}$  and  $^1\text{H}$  hyperfine constants and Lande  $g$  factors. In contrast, the higher energy subband exhibits very *small* Lande  $g$  factors and hyperfine constants, which is explained within a model that incorporates only the  $\tilde{A}^1A''$ – $\tilde{X}^1A'$  interaction. We thus demonstrate that polarization quantum beat spectra provides efficient discrimination between RT and spin–orbit interactions. Analysis of the lower energy subband in concert with *ab initio* electronic structure calculations has yielded the first information on the  $^{19}\text{F}$  and  $^1\text{H}$  hyperfine structure of the  $\tilde{a}^3A''$  state and the magnitude of the spin–orbit matrix elements. © 2004 American Institute of Physics. [DOI: 10.1063/1.1803530]

### I. INTRODUCTION

Simple carbenes continue to attract significant interest due to the important role they play in many areas of chemistry.<sup>1–11</sup> As the smallest carbene with a singlet ground state, HCF is a prototype for understanding the electronic spectroscopy and structure of singlet carbenes.<sup>12–34</sup> The  $\tilde{A}^1A'' \leftarrow \tilde{X}^1A'$  system has been studied in some detail, first by Merer and Travis,<sup>23</sup> and subsequently by Hirota and co-workers,<sup>24–28</sup> Kable and co-workers,<sup>29,30</sup> and by our group.<sup>31–33</sup> A significant motivation for our studies is to obtain information on the  $\tilde{a}^3A''$  state, which is difficult to probe directly but can be evidenced via perturbations. Indeed, Hirota and co-workers identified local singlet-triplet perturbations in the  $0_0^0$  band by their large Zeeman effects, up to  $1\mu_B$ , although a quantitative analysis was not achieved.<sup>27,28</sup> In contrast, the Zeeman effect of unperturbed levels was typically no greater than  $0.05\mu_B$ .<sup>27,28</sup>

In the preceding paper,<sup>34</sup> as well as previous reports,<sup>32,33</sup> we examined unperturbed levels the  $\tilde{A}^1A'' \leftarrow \tilde{X}^1A'$  system using polarization quantum beat spectroscopy. The intrinsically high resolution of quantum beat spectra (QBS) allowed us to resolve both the  $^{19}\text{F}$  and  $^1\text{H}$  hyperfine structure in the  $\tilde{A}^1A''$  state, which was probed as a function of vibrational level.<sup>32,34</sup> In addition, Zeeman quantum beat spectroscopy was used to determine the weak field Lande  $g_{aa}$  factors,<sup>34</sup> which for unperturbed levels range from 0.010 to 0.095.

Consistent with a model that incorporates only the  $\tilde{A}^1A''$ – $\tilde{X}^1A'$  interaction, the majority of vibrational levels exhibit a linear correlation of  $C_{aa}$  and  $g_{aa}$ , and our analysis yielded effective ( $\tilde{a}$ ) hyperfine constants for the  $^{19}\text{F}$  and  $^1\text{H}$  nuclei (in MHz) of 728(23) and 55(2), respectively.<sup>34</sup>

In this paper, we focus on perturbations in the HCF  $\tilde{A}^1A'' \leftarrow \tilde{X}^1A'$  system. Specifically, we show via a detailed analysis of the  $K_a = 1 \leftarrow 0$  subband of  $2_0^4$ , where both Renner–Teller (RT) and spin–orbit interactions are operative, that hyperfine and Zeeman spectroscopy are a sensitive probe of perturbations in this system. Our analysis, in combination with *ab initio* electronic structure calculations, has provided the first glimpse into the spectroscopic properties of the triplet state and the magnitude of the spin–orbit matrix elements.

### II. EXPERIMENTAL SECTION

The apparatus, pulsed discharge nozzle, and data acquisition procedures have previously been described in detail.<sup>31–37</sup> Briefly, HCF was generated in a pulsed electrical discharge through a  $\sim 2\%$  mixture of  $\text{CH}_2\text{F}_2$  (Aldrich, 99.9%) in argon. The laser system consisted of an etalon narrowed dye laser (Lambda-Physik Scanmate 2E) operating on Coumarin 307 dye, pumped by the second or third harmonic of an injection seeded Nd:YAG laser (Continuum Powerlite 7010), where YAG stands for yttrium aluminum garnet. The laser wavelength was calibrated using optogalvanic spectroscopy in a Fe–Ne or Fe–Ar hollow cathode lamp. The experimental procedures for acquiring fluores-

<sup>a)</sup> Author to whom correspondence should be addressed. Electronic mail: scott.reid@mu.edu

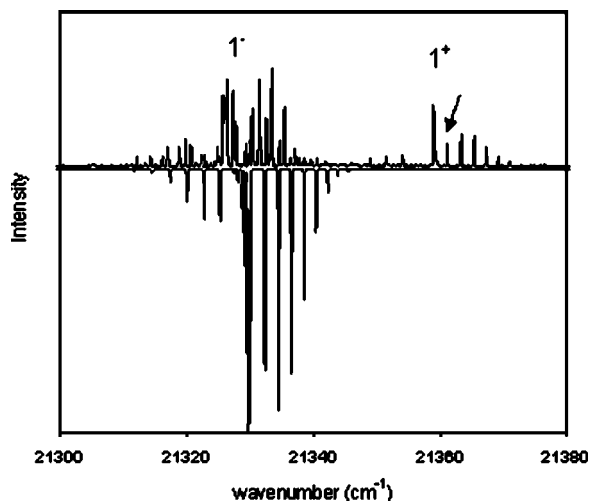


FIG. 1. Experimental (top) and simulated fluorescence excitation spectra of the  $K_a' = 1 \leftarrow 0$  subband of  $2_0^4$ . The two split subbands in the experimental spectrum are labeled “ $1^-$ ” and “ $1^+$ ,” and this notation is used throughout the text. An arrow marks the position of the  ${}^rR_0(0)$  transition of the higher energy subband ( $1^+$ ), the quantum beat spectrum of which is shown in Fig. 2.

cence excitation and polarization quantum beat spectra, and fluorescence lifetime measurements, are the same as those described in previous work.

### III. RESULTS AND DISCUSSION

Figure 1 displays a laser induced fluorescence spectrum of the region of the  $K_a = 1 \leftarrow 0$  subband of  $2_0^4$ , together with a simulated spectrum generated from the rotational constants determined by fitting unperturbed lines in the  $K_a = 0 \leftarrow 1$  and  $2 \leftarrow 1$  subbands.<sup>33</sup> Two  $K_a = 1 \leftarrow 0$  subbands are clearly observed, a situation similar to that found for  $2_0^1$ , where the perturbation was assigned to the Renner–Teller interaction with a high vibrational level of  $\tilde{X}^1A'$ , and a coupling matrix element  $\langle \tilde{A}^1A''(2^1) | AL_a | \tilde{X}^1A'(v'') \rangle = 1.4465(58) \text{ cm}^{-1}$  was derived.<sup>27</sup> While the higher energy subband is free of rotational perturbations, almost every line in the lower energy subband is rotationally perturbed, as evidenced by the presence of many extra lines (Fig. 1). For both subbands, a pronounced lengthening of the fluorescence lifetime is observed compared to unperturbed rotational lines in the  $K_a = 0 \leftarrow 1$  subband (Table I). As we will show, the large splitting is consistent with the Renner–Teller interaction, while the extensive rotational perturbations in the lower energy subband predominantly arise from spin–orbit interactions with  $\tilde{a}^3A''$ .

We began our analysis by deriving the matrix element associated with the splitting of the  $K_a' = 1$  level. The unperturbed position of this subband was determined from our fit (Fig. 1), and as the higher energy subband (hereafter denoted  $1^+$ ) was not rotationally perturbed, a direct fit was performed to determine the origin. A fit of the lower energy subband (hereafter referred to as  $1^-$ ) was obviously not possible, and we derived the origin by fitting three apparently unperturbed high  $J$  lines in the  ${}^rR_0$  branch, using the rotational constant of the higher energy subband. The relative band intensities were determined by summing over all ob-

TABLE I. Fluorescence lifetimes measured for the  $2^4$  band.

Transition		Lifetime ( $\mu\text{s}$ ) <sup>a</sup>
$K = 0$	${}^pQ_1 \text{ head}$	1.552(11)
	${}^pR_1(1)$	1.539(10)
	${}^pR_1(2)$	1.538(8)
$K = 1 \text{ (lower)}$	${}^rQ_0(1)^+$	5.870(47)
	${}^rR_0(1)^-$	5.228(43)
	${}^rR_0(1)^+$	3.796(5)
	${}^rR_0(2)^-$	6.75(19)
	${}^rR_0(2)^+$	3.676(61)
	${}^rQ_0 \text{ head}$	4.815(25)
$K = 1 \text{ (upper)}$	${}^rR_0(0)$	4.827(21)
	${}^rR_0(1)$	5.396(52)
	${}^rR_0(2)$	4.442(77)

<sup>a</sup>One standard error in parentheses.

served lines and subtracting off the baseline, which yielded a ratio  $1^+/1^- = 0.206(8)$ . Using the formulas that result from two-level perturbation theory,<sup>33</sup> we derive a coupling matrix element  $\langle \tilde{A}^1A''(2^4) | AL_a | \tilde{X}^1A'(v'') \rangle = 6.1(11) \text{ cm}^{-1}$ , approximately four times that found for  $2^1$ .<sup>27</sup> This is not surprising, given that the  $A$  rotational constant of  $2^4$  is approximately twice that of  $2^1$ .<sup>33</sup>

Supporting evidence in favor of the RT hypothesis for the subband splitting comes from polarization quantum beat measurements. We have previously shown that the  $2^1$  band, which is perturbed by a high lying vibrational level of  $\tilde{X}^1A'$ , exhibits smaller  ${}^{19}\text{F}$  (and  ${}^1\text{H}$ ) hyperfine constants than expected from theory.<sup>33</sup> The same is true here, as shown in the upper panel of Fig. 2, which displays the spectrum obtained for the  ${}^rR_0(0)$  line of  $1^+$  (marked with an arrow in Fig. 1). Our analysis gives  $C_{aa}({}^{19}\text{F}) = -7.206(39)$  and  $C_{aa}({}^1\text{H}) = -0.434(44)$ , which are among the smallest values observed for any level in the  $\tilde{A}^1A''$  state.<sup>32,34</sup> The former may be compared with a value of  $C_{aa}({}^{19}\text{F}) = -50 \text{ MHz}$  predicted for the unperturbed  $2^4$  level from the trend observed for the  $2^2$  and  $2^3$  levels.<sup>32,34</sup>

To understand the origin of the small hyperfine constants for  $1^+$ , we consider that, neglecting small terms arising from closed shell electrons and other nuclei, and assuming that only  $\tilde{X}^1A'$  state levels contribute to the sum,<sup>28</sup> the nuclear spin/overall rotation constant  $C_{aa}$  in the  $\tilde{A}^1A''$  state is expressed as<sup>28,38</sup>

$$C_{aa}(v') = -4 \sum_{v''} \frac{\langle \tilde{A}, v' | aL_a | \tilde{X}, v'' \rangle \langle \tilde{X}, v'' | AL_a | \tilde{A}, v' \rangle}{E_{v'} - E_{v''}}. \quad (1)$$

Using effective hyperfine and rotation constants, Eq. (1) is rewritten as

$$C_{aa}(v') = -4\bar{a}\bar{A} \sum_{v''} \frac{\langle \tilde{A}, v' | L_a | \tilde{X}, v'' \rangle^2}{E_{v'} - E_{v''}}. \quad (2)$$

Barring any near resonance, the dominant terms in this sum will have  $E_{v'} > E_{v''}$ , leading to a negative  $C_{aa}$ , as is indeed observed for low-lying levels in the  $\tilde{A}^1A''$  state.<sup>28,32,34</sup> How-

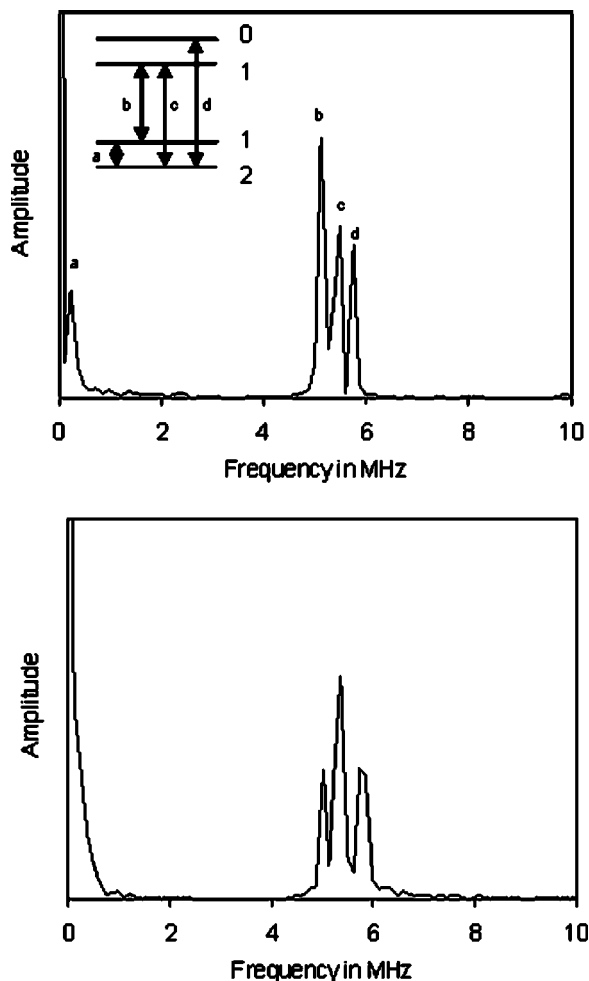


FIG. 2. Upper panel. Experimental zero-field polarization quantum beat spectrum of the  ${}^7R_0(0)$  transition of the higher energy subband ( $1^+$ ), marked with an arrow in Fig. 1. Assignments of the quantum beats follow the energy level diagram shown in terms of the F quantum number. Lower panel. Zeeman quantum beat spectrum of the same transition taken at a field strength of 20.38 G.

ever, when a near resonance occurs with a *higher* lying level of  $\tilde{X}^1A'$ , that term will contribute *positively* to the sum, resulting in a partial cancellation. To estimate the contribution of this term for  $2^4$ , we use the matrix element derived above, an effective rotational constant  $\bar{A}$  equal to the average of the fit value for  $2^4$  (51.8  $\text{cm}^{-1}$ ) and the  $0_0$  level of  $\tilde{X}^1A'$ ,<sup>23–25,33,34</sup> our previously derived value of  $\bar{a}$  for the  ${}^{19}\text{F}$  nucleus,<sup>34</sup> and the estimated separation ( $\sim 24.8 \text{ cm}^{-1}$ ) of the zeroth-order levels determined from the deperturbation analysis. Inputting these into Eq. (2), we calculate a contribution of  $\sim +56 \text{ MHz}$  to  $C_{aa}$ , which is clearly of the correct magnitude to offset the expected contribution from lower-lying  $\tilde{X}^1A'$  state levels.

A similar analysis may be applied to the Zeeman effect of  $1^+$ . Using the predicted value of  $C_{aa}({}^{19}\text{F}) = -50 \text{ MHz}$ , we estimate the Landé  $g_{aa}$  factor of the *unperturbed*  $2^4$  level as<sup>34</sup>

$$\begin{aligned} g_{aa} &= -C_{aa}({}^{19}\text{F})/\bar{a}({}^{19}\text{F}) \\ &= -(-50 \text{ MHz})/(728 \text{ MHz}) = 0.07. \end{aligned}$$

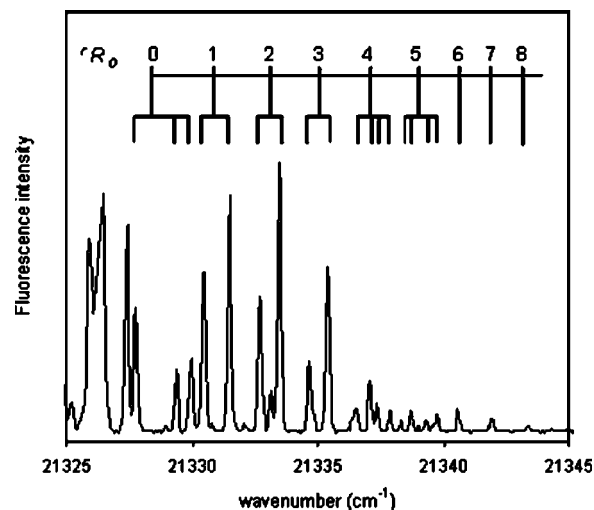


FIG. 3. Expanded view of the  ${}^7R_0$  lines in the lower energy subband ( $1^-$ ), showing the assigned perturbation patterns.

In contrast, as shown in the lower panel of Fig. 2, the Zeeman splittings in the quantum beat spectrum of the  ${}^7R_0(0)$  line of  $1^+$  are not resolved even at a field of 20.38 G, and we can only place an upper limit on  $g_{aa}$  of  $\sim 0.002$ . When Eq. (1) is valid, the corresponding Landé  $g_{aa}$  factor is given by<sup>28</sup>

$$g_{aa}(v') = 4 \sum_{v''} \frac{\langle \tilde{A}, v' | L_a | \tilde{X}, v'' \rangle \langle \tilde{X}, v'' | A L_a | \tilde{A}, v' \rangle}{E_{v'} - E_{v''}}, \quad (3)$$

which may be simplified in the manner used above to

$$g_{aa}(v') = 4\bar{A} \sum_{v''} \frac{\langle \tilde{A}, v' | L_a | \tilde{X}, v'' \rangle^2}{E_{v'} - E_{v''}}. \quad (4)$$

Inputting the values derived above into Eq. (4), we estimate a contribution to  $g_{aa}$  of  $\sim -0.08$ , which again is of the correct magnitude to produce the small observed Zeeman effect.

We now turn to the lower energy subband  $1^-$ . Figure 3 displays an expanded view of the  ${}^7R_0$  branch of this subband, showing the rotational assignments and perturbation patterns, which were assigned wherever possible using combination differences. The assignments for  ${}^7R_0(4)$ – ${}^7R_0(5)$  are speculative due to the low intensity of the corresponding lines in the  ${}^7P_0$  branch. All excited state levels with  $J \leq 5$  are perturbed by at least one background level, and the  ${}^7R_0(0)$  line is split into three lines, indicating a perturbation by more than one background level. As a first step towards identifying the perturbing level(s), we employed hyperfine and Zeeman QBS. Figure 3 displays the zero-field polarization QBS spectra for the three  ${}^7R_0(0)$  lines. Although the familiar four-line pattern is reproduced in each case, the splittings are much larger than obtained for any other  $\tilde{A}^1A''$  level.<sup>32,34</sup> Similar behavior is found in the Zeeman effect. The three lines exhibit Landé  $g_J$  factors of 0.648(5), 0.127(3), and 0.137(3), which are two to five times larger than expected for the unperturbed  $2^4$  level, and *two orders of magnitude* larger than observed for the  ${}^7R_0(0)$  line in the  $1^+$  subband. These findings implicate spin–orbit mixing with levels of the  $\tilde{a}^3A''$  state.

Previously, Hirota and co-workers identified spin–orbit mixing for isolated rotational levels in  $2^1$  via large Zeeman

TABLE II. Calculated and experimental isotropic hyperfine constants (in MHz) for  $\text{CH}_2(\bar{X}^3A_1)$ .

Method	Basis set	$a_F(^{13}\text{C})$	$a_F(^1\text{H})$
B3LYP	6-31G(d)	260.9	-17.1
	6-311G(d,p)	225.7	-12.8
	cc-pVTZ	200.3	-11.0
	EPR-III	236.5	-12.6
QCISD	6-311G(d,p)	304.4	-59.4
	cc-pVTZ	267.0	-56.8
	EPR-III	309.6	-59.1
CCSD(T)	6-31G(d)	333.6	-68.4
	6-311G(d,p)	304.4	-58.5
	cc-pVTZ	267.0	-56.8
	EPR-III	309.6	-59.1
	Experiment		
Reference 42		247	
Reference 43		245	
Reference 44		249	
Reference 45		238.7(555)	
Reference 46			-20.26(51)
Reference 47			-12.48(90)
Reference 48			-13.62(86)
Reference 49			-16.81(28)

effects, up to  $\sim 1\mu_B$ , although a quantitative analysis was not achieved.<sup>27,28</sup> Of course, the goal of deperturbation analysis is to gain quantitative information on the  $\bar{a}^3A''$  state and the magnitude of the spin-orbit coupling matrix elements. This is complicated here by a lack of knowledge concerning the perturbing level(s). For example, considering the  $1_{10}$  level accessed via the  ${}^7R_0(0)$  transition, mixing is allowed under a  $\Delta J=0$  selection rule with  $\bar{a}^3A''$  levels having  $N=0, 1$ , or  $2$  and  $K=0-N$ . Moreover,  $K$ -type doubling must be considered for levels with  $K \geq 1$ , giving nine possibilities for the quantum numbers of the perturbing state. To restrict this range, we must assume that the observed hyperfine structure and Zeeman effect is due entirely to the triplet character of the perturbed levels. Given the very small hyperfine splittings and Zeeman effect observed for  $1^+$ , we expect this approximation to be valid to within a few percent. For example, the sum of the observed Lande  $g_J$  factors for the three  ${}^7R_0(0)$  lines is 0.911(7), which may be compared to the ex-

pected  $g_J$  factor of a pure triplet level of 2.002 ( $J=1, N=0$ ) or 1.001 ( $J=1, N=1, 2$ ). This suggests the presence of a single perturbing  $\bar{a}^3A''$  level with  $N=1$  or  $2$ .

To gain further insight, we turned to the measured hyperfine splittings, in concert with *ab initio* calculations of the triplet state hyperfine constants. A review of the literature revealed relatively few calculations of the hyperfine constants of triplet carbenes.<sup>39-41</sup> Given that no experimental data exist for the hyperfine constants of  $\text{HCF}(\bar{a}^3A'')$ , we used the simplest triplet carbene, methylene ( $\text{CH}_2$ ), as a benchmark to assess the reliability of various methods and basis sets. The full results of these calculations will be reported elsewhere; however, a selection of the calculated isotropic hyperfine constants are compared in Table II with available experimental data.<sup>42-49</sup> Good agreement is found using B3LYP with large basis sets on the equilibrium geometry optimized at the B3LYP/6-311+G(3df) level, which was in close agreement with experiment [ $r_{\text{CH}}=1.081 \text{ \AA}$  (calc) versus,  $1.08 \text{ \AA}$  (expt),  $\theta_{\text{HCH}}=134.7^\circ$  (calc) versus  $135^\circ$  (expt)].<sup>42</sup> We note that the B3LYP functional has successfully been used to reproduce hyperfine coupling constants of open shell species.<sup>50</sup> In Table III, we compare with experiment the results for the anisotropic constants, calculated at the B3LYP/EPR-III level, which again are in reasonable agreement with experiment.

We subsequently computed the  $^{19}\text{F}$  and  $^1\text{H}$  hyperfine constants for the  $\bar{a}^3A''$  level of HCF at the B3LYP/EPR-III level using the optimized B3LYP/EPR-III geometry [ $r_{\text{CH}}=1.089 \text{ \AA}$ ,  $r_{\text{CF}}=1.313 \text{ \AA}$ ,  $\theta_{\text{HCF}}=121.8^\circ$ ], which is similar to that determined previously using coupled-cluster theory at the RCCSD(T)/cc-pVQZ level.<sup>51</sup> The calculated hyperfine constants are (in MHz)

$$\begin{aligned}
 a_F(^{19}\text{F}) &= 200.1, & a_F(^1\text{H}) &= 95.4, \\
 T_{xx}(^{19}\text{F}) &= -514.4, & T_{xx}(^1\text{H}) &= -52.8, \\
 T_{yy}(^{19}\text{F}) &= 254.4, & T_{yy}(^1\text{H}) &= -21.7, \\
 T_{zz}(^{19}\text{F}) &= 260.1, & T_{zz}(^1\text{H}) &= 74.5.
 \end{aligned}$$

Rather than attempting a direct fit of the experimental data, which would require at least six hyperfine parameters, we used the calculated constants to predict the expected hyper-

TABLE III. Calculated and experimental anisotropic hyperfine constants (in MHz) for  $\text{CH}_2(\bar{X}^3A_1)$ . The theoretical results have been transformed to the inertial axis frame.

	$^{13}\text{C}$ constants			$^1\text{H}$ constants			
	$T_{aa}$	$T_{bb}$	$T_{cc}$	$T_{aa}$	$T_{bb}$	$T_{cc}$	
Calculated	-119.7	59.3	60.4	48.5	-19.5	-32.0	
B3LYP EPR-III							
		Experiment					
Reference 42	(-)70	34	35				
Reference 43	(-)63	34	30				
Reference 44	(-)53	31	25				
Reference 45	-65(22)	33(22)	a				
Reference 46				39.7(17)	-20.2(19)	a	
Reference 47				42.09(98)	-21.4	a	
Reference 48				43.68(87)	-21.9(12)	a	
Reference 49				32.32(21)	-20.70(36)	a	

<sup>a</sup> $T_{bb} - T_{cc} = 0$  (assumed).

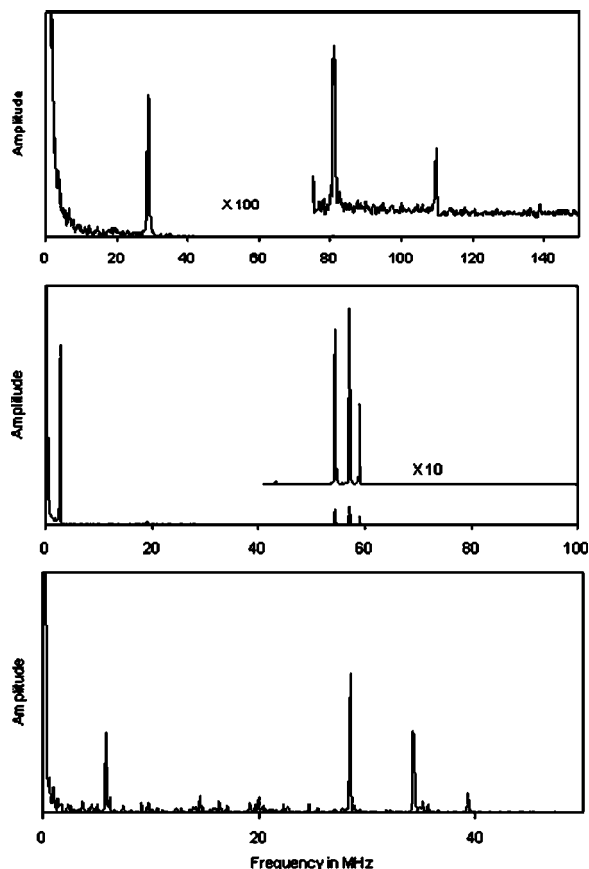


FIG. 4. Zero-field quantum beat spectra of the three  ${}^1R_0(0)$  lines in the lower energy subband ( $1^-$ ). The spectra are arranged (top to bottom) in order of increasing energy of the corresponding transitions.

fine level splittings for the pure triplet state, employing a standard triplet state Hamiltonian<sup>52,53</sup> with matrix elements evaluated in a case  $b_{\beta I}$  basis,<sup>52–56</sup> where  $\mathbf{J}=\mathbf{N}+\mathbf{S}$ ,  $\mathbf{F}_1=\mathbf{J}+\mathbf{I}_F$ , and  $\mathbf{F}=\mathbf{F}_1+\mathbf{I}_H$ .

We estimated the pure triplet hyperfine splittings from the experimental data using two approaches. The first followed that of Huber and co-workers, who used a two-level model of singlet-triplet coupling in propynal to show that the beat frequencies associated with the pure triplet level equals the sum of beat frequencies of the eigenstates, when  $F_1$  and  $J$  remain good quantum numbers and the hyperfine splitting comes solely from the triplet state.<sup>53</sup> Accounting for the experimental response function, the beat patterns observed in Fig. 4 closely resemble those calculated in the case  $b$  basis,<sup>34</sup> suggesting that  $F_1$  and  $J$  are good quantum numbers. In method I then, we simply summed the beat frequencies for the components of each  ${}^1R_0$  line. In method II, the observed Landé factor of each  ${}^1R_0$  line was taken as a measure of the triplet state character, with the sum of Landé factors used to identify the likely  $N$  value of the perturbing triplet level. We then scaled the observed hyperfine splittings accordingly, and averaged the values for all components of each  ${}^1R_0$  line. We compare in Table IV the calculated level splittings (beat frequencies) of the pure triplet state with  $J=1$  for different values of  $N$ ,  $K$  with the results from these two approaches (denoted “sum” and “scaled”) applied to the three  ${}^1R_0(0)$

TABLE IV. Calculated and experimental beat frequencies (in MHz) for CHF ( $\tilde{a}^3A''$ ,  $J=1$ ).

	Beat frequencies (MHz) <sup>a</sup>			
	$\omega_1$	$\omega_2$	$\omega_3$	$\omega_4$
	Experiment			
<i>Sum</i>	37.4	163.8	201.2	237.2
<i>Scaled</i>	33.1	231.4	264.6	293.7
	Calculated			
$N=0, K=0$	117.0	209.2	326.2	443.3
$N=1, K=0$	42.6	51.6	94.2	170.4
$N=1, K=1$	37.5	223.9	261.3	311.1
$N=2, K=0$	38.4	348.5	386.9	400.6
$N=2, K=1$	49.8	223.9	273.7	311.1
$N=2, K=2$	42.6	76.2	118.8	170.4

<sup>a</sup>Beat frequency assignments follow the notation used in Fig. 2.

lines. Reasonable agreement is observed with two levels:  $N=1, K=1$ , and  $N=2, K=1$ .

To gain further insight, we extended this analysis to the higher  ${}^1R_0$  lines of the  $1^-$  subband, which provide a consistent picture of spin-orbit mixing with  $\tilde{a}^3A''$ . For example, the two  ${}^1R_0(2)$  lines exhibit Landé  $g_J$  factors of 0.0962(11) and 0.0471(6), respectively. The sum of the Landé factors, 0.1433(13), is consistent with the  $g_J$  of 0.167 expected for a pure triplet level with  $J=N=3$ . Moreover, the triplet character predicted from the Landé  $g_J$  factors [58% for the first component, 28% for the second] is consistent with that inferred from the fluorescence lifetimes (52% and 35%). Unlike the case of  ${}^1R_0(0)$ , only two of the four distinct beat frequencies appear with appreciable intensity in the zero-field quantum beat spectrum. The sum of zero-field frequencies for the two split lines of  ${}^1R_0(2)$  are, respectively, 10.2 and 25.6 MHz. Using the scaled approach, we derive values of 9.6 and 25.8 MHz. These may be compared with predicted values of 9.0 and 35.8 MHz for a triplet level with  $J=N=3$  and  $K=1$ . Thus, the general picture which emerges from our analysis is that the  $1^-$  subband is perturbed by a background  $\tilde{a}^3A''$  level under the selection rule  $\Delta N=\Delta K=0$ .

Information on the magnitude of the spin-orbit matrix elements may be gleaned from the  ${}^1R_0(1)$ - ${}^1R_0(3)$  lines, each of which appear to be perturbed by a single background level. Using a two-level deperturbation analysis,<sup>33</sup> we derive matrix elements of, respectively, 0.51(16), 0.41(13), and 0.38(12)  $\text{cm}^{-1}$  for these levels. We hesitate to infer a rotational state dependence from just three lines, but note that the observed trend is certainly not inconsistent with the predicted  $[J(J+1)]^{-1/2}$  dependence under the selection rule  $\Delta N=\Delta K=0$ .<sup>57</sup> A matrix element of similar magnitude [ $W_{ST}=0.651(7)$   $\text{cm}^{-1}$ ] was reported by Clouthier and co-workers for vibronic spin-orbit coupling in the  $\tilde{A}^1A_2$  state of  $\text{H}_2\text{CS}$ .<sup>58</sup> We cannot differentiate between a vibronic and direct mechanism, given a lack of information on the perturbing triplet level and the similar rotational state dependence of the coupling matrix elements.<sup>57</sup>

Finally, we should point out that the perturbations in this band are a clear example of a doorway-type interaction.<sup>33,59–62</sup> The energy of the  $2^4$  band lies only  $\sim 16\,000$   $\text{cm}^{-1}$  above the predicted position of the  $\tilde{a}^3A''$  state

minimum,<sup>14,15,51,63–65</sup> ensuring that the triplet level density is sparse, and thus it is not surprising that only one of the RT split subbands is perturbed by spin–orbit interactions. It is highly desirable to probe such interactions on the ground state surface, and experiments toward that end are currently planned.

## ACKNOWLEDGMENTS

We gratefully acknowledge the donors of the Petroleum Research Fund of the American Chemical Society and the National Science Foundation (Grant No. CHE-0353596) for support of this research, and thank Dr. Ju Xin for useful discussions.

- <sup>1</sup> *Carbenes*, edited by R. A. Moss and M. Jones, Jr., Reactive Intermediates in Organic Chemistry Series Vol. I (Wiley-Interscience, New York, 1973); Reactive Intermediates in Organic Chemistry Series Vol. II (Wiley-Interscience, New York, 1975).
- <sup>2</sup> W. Kirmse, *Carbene Chemistry*, 2nd ed. (Academic, New York, 1971).
- <sup>3</sup> J. C. Sciano, *Handbook of Organic Photochemistry* (CRC Press, Boca Raton, FL, 1989), Vol. 2, Chap. 9.
- <sup>4</sup> F. A. Carey and R. J. Sundberg, *Advanced Organic Chemistry*, 3rd ed. (Plenum, New York, 1990), Pt. 3.
- <sup>5</sup> U. E. Weirsum and L. W. Jenneskens, in *Gas Phase Reactions in Organic Synthesis*, edited by Y. Vallée (Gordon and Breach, Australia, 1997).
- <sup>6</sup> A. M. Dean and J. W. Bozzelli, in *Gas-phase Combustion Chemistry*, edited by W. C. Gardiner, Jr., (Springer, New York, 2000), Chap. 2.
- <sup>7</sup> G. B. Bacskay, M. Martoprawiro, and J. C. Mackie, *Chem. Phys. Lett.* **290**, 391 (1998).
- <sup>8</sup> K. Sendt, E. Ikeda, G. B. Bacskay, and J. C. Mackie, *J. Phys. Chem. A* **103**, 1054 (1999).
- <sup>9</sup> M. Martoprawiro, G. B. Bacskay, and J. C. Mackie, *J. Phys. Chem. A* **103**, 3923 (1999).
- <sup>10</sup> K. Sendt, G. B. Bacskay, and J. C. Mackie, *J. Phys. Chem. A* **104**, 1861 (2000).
- <sup>11</sup> R. P. Wayne, *Chemistry of Atmospheres* (Oxford University Press, Oxford, 1991), Chap. 8, and references therein.
- <sup>12</sup> E. A. Carter and W. A. Goddard III, *J. Chem. Phys.* **88**, 1752 (1988).
- <sup>13</sup> C. W. Bauschlicher, Jr., H. F. Schaefer III, and P. S. Bagus, *J. Am. Chem. Soc.* **99**, 7106 (1977).
- <sup>14</sup> G. E. Scseria, M. Durán, R. G. A. R. MacLagan, and H. F. Schaefer III, *J. Am. Chem. Soc.* **108**, 3248 (1986).
- <sup>15</sup> K. K. Irikura, W. A. Goddard III, and J. L. Beauchamp, *J. Am. Chem. Soc.* **114**, 48 (1992).
- <sup>16</sup> E. A. Carter and W. A. Goddard III, *J. Phys. Chem.* **91**, 4651 (1987).
- <sup>17</sup> S. K. Shin, W. A. Goddard III, and J. L. Beauchamp, *J. Chem. Phys.* **93**, 4986 (1990).
- <sup>18</sup> G. L. Gutsev and T. Ziegler, *J. Phys. Chem.* **95**, 7220 (1991).
- <sup>19</sup> N. Russo, E. Sicilia, and M. Toscano, *J. Chem. Phys.* **97**, 5031 (1992).
- <sup>20</sup> B. Weis, P. Rosmus, K. Yamashita, and K. Morokuma, *J. Chem. Phys.* **92**, 6635 (1990).
- <sup>21</sup> T. W. Schmidt, G. B. Bacskay, and S. H. Kable, *Chem. Phys. Lett.* **292**, 80 (1998).
- <sup>22</sup> R. I. Patel, G. W. Stewart, K. Casleton, J. L. Gole, and J. R. Lombardi, *Chem. Phys.* **52**, 461 (1980).
- <sup>23</sup> A. J. Merer and D. N. Travis, *Can. J. Phys.* **44**, 1541 (1966).
- <sup>24</sup> M. Kakimoto, S. Saito, and E. Hirota, *J. Mol. Spectrosc.* **88**, 300 (1981).
- <sup>25</sup> T. Suzuki, S. Saito, and E. Hirota, *J. Mol. Spectrosc.* **90**, 447 (1981).
- <sup>26</sup> R. J. Butcher, S. Saito, and E. Hirota, *J. Chem. Phys.* **80**, 4000 (1984).
- <sup>27</sup> T. Suzuki, S. Saito, and E. Hirota, *Can. J. Phys.* **62**, 1328 (1984).
- <sup>28</sup> T. Suzuki and E. Hirota, *J. Chem. Phys.* **85**, 5541 (1986).
- <sup>29</sup> T. W. Schmidt, G. B. Bacskay, and S. H. Kable, *J. Chem. Phys.* **110**, 11277 (1999).
- <sup>30</sup> K. Nauta, J. S. Guss, N. L. Owens, and S. H. Kable, *J. Chem. Phys.* **120**, 3517 (2004).
- <sup>31</sup> H. Fan, I. Ionescu, C. Annesley, and S. A. Reid, *Chem. Phys. Lett.* **378**, 548 (2003).
- <sup>32</sup> I. Ionescu, H. Fan, C. Annesley, J. Xin, and S. A. Reid, *J. Chem. Phys.* **120**, 1164 (2004).
- <sup>33</sup> H. Fan, I. Ionescu, C. Annesley, J. Cummins, M. Bowers, J. Xin, and S. A. Reid, *J. Phys. Chem. A* **108**, 3732 (2004).
- <sup>34</sup> H. Fan, I. Ionescu, J. Xin, and S. A. Reid, *J. Chem. Phys.*, **121**, ■ (2004).
- <sup>35</sup> J. Xin, I. Ionescu, D. Kuffel, and S. A. Reid, *Chem. Phys.* **291**, 61 (2003).
- <sup>36</sup> J. Xin, I. Ionescu, H. Fan, and S. A. Reid, *Rec. Res. Develop. Chem. Phys.* **5**, 211 (2004).
- <sup>37</sup> J. Xin, H. Fan, I. Ionescu, C. Annesley, and S. A. Reid, *J. Mol. Spectrosc.* **219**, 37 (2003).
- <sup>38</sup> C. H. Townes and A. L. Schawlow, *Microwave Spectroscopy* (McGraw-Hill, New York, 1955), Chap. 8.
- <sup>39</sup> Y. J. I'Haya, T. Morikawa, and J. Nakano, *Int. J. Quantum Chem., Quantum Chem. Symp.* **13**, 205 (1979).
- <sup>40</sup> T. Morikawa, Y. J. I'Haya, and J. Nakano, *Bull. Chem. Soc. Jpn.* **53**, 878 (1980).
- <sup>41</sup> H. Nakatsuji, M. Ehara, and T. Momose, *J. Chem. Phys.* **100**, 5821 (1994).
- <sup>42</sup> E. Wasserman, V. J. Kuck, R. S. Hutton, E. D. Anderson, and W. A. Yager, *J. Chem. Phys.* **54**, 4120 (1971).
- <sup>43</sup> R. A. Bernheim, H. W. Bernard, P. S. Wang, L. S. Wood, and P. S. Skell, *J. Chem. Phys.* **54**, 3223 (1971).
- <sup>44</sup> R. A. Bernheim, T. Adl, H. W. Bernard, A. Songco, P. S. Wang, R. Wang, L. S. Wood, and P. S. Skell, *J. Chem. Phys.* **64**, 2747 (1976).
- <sup>45</sup> A. R. W. McKellar and T. J. Sears, *Can. J. Phys.* **61**, 480 (1983).
- <sup>46</sup> T. J. Sears, P. R. Bunker, A. R. W. McKellar, K. M. Evenson, D. A. Jennings, and J. M. Brown, *J. Chem. Phys.* **77**, 5348 (1982).
- <sup>47</sup> F. J. Lovas, R. D. Suenram, and K. M. Evenson, *Astrophys. J.* **267**, L131 (1983).
- <sup>48</sup> H. Ozeki and S. Saito, *J. Chem. Phys.* **104**, 2167 (1996).
- <sup>49</sup> E. A. Michael, F. Lewen, G. Winnewisser, H. Ozeki, H. Habara, and E. Herbst, *Astrophys. J.* **596**, 1356 (2003).
- <sup>50</sup> V. Barone, in *Recent Advances in Density Functional Theory*, Vol. 1, edited by D. P. Chong (World Scientific, Singapore, 1996).
- <sup>51</sup> T. W. Schmidt, G. B. Bacskay, and S. H. Kable, *Chem. Phys. Lett.* **292**, 80 (1998).
- <sup>52</sup> W. T. Raynes, *J. Chem. Phys.* **41**, 3020 (1964).
- <sup>53</sup> H. Bitto, M. P. Docker, P. Schmidt, and J. R. Huber, *J. Chem. Phys.* **92**, 187 (1990).
- <sup>54</sup> J. M. Cook, G. W. Hills, and R. F. Curl, Jr., *J. Chem. Phys.* **67**, 1450 (1977).
- <sup>55</sup> C. Yamada, Y. Endo, and E. Hirota, *J. Chem. Phys.* **79**, 4159 (1983).
- <sup>56</sup> *High Resolution Spectroscopy of Transient Molecules*, edited by E. Hirota (Springer, Berlin, 1985), Chap. 4.
- <sup>57</sup> C. G. Stevens and J. C. D. Brand, *J. Chem. Phys.* **58**, 3324 (1973).
- <sup>58</sup> D. J. Clouthier, D. A. Ramsay, and F. W. Birss, *J. Chem. Phys.* **79**, 5851 (1983).
- <sup>59</sup> J. Go and D. S. Perry, *J. Chem. Phys.* **97**, 6994 (1992).
- <sup>60</sup> A. McIlroy, D. J. Nesbitt, E. R. Th. Kerstel, B. H. Pate, K. K. Lehmann, and G. Scoles, *J. Chem. Phys.* **100**, 2596 (1994).
- <sup>61</sup> S. Cupp, C. Y. Lee, D. McWhorter, and B. H. Pate, *J. Chem. Phys.* **109**, 4302 (1998).
- <sup>62</sup> O. V. Boyarkina, T. R. Rizzo, and D. S. Perry, *J. Chem. Phys.* **110**, 11346 (1999).
- <sup>63</sup> A. Gobbi and G. Frenking, *J. Chem. Soc., Chem. Commun.* **14**, 1162 (1993).
- <sup>64</sup> V. M. Garcia, O. Castell, M. Reguero, and R. Callol, *Mol. Phys.* **87**, 1395 (1996).
- <sup>65</sup> M. K. Gilles, K. M. Ervin, J. Ho, and W. C. Lineberger, *J. Phys. Chem.* **96**, 1130 (1992).